

Ultrafast carrier dynamics in SnOx thin films

Zhong-guo Li, Lingyan Liang, Hongtao Cao, Zhengguo Xiao, Xingzhi Wu, Yu Fang, Junyi Yang, Tai-Huei Wei, and Ying-lin Song

Citation: [Applied Physics Letters](#) **106**, 102103 (2015); doi: 10.1063/1.4914546

View online: <http://dx.doi.org/10.1063/1.4914546>

View Table of Contents: <http://scitation.aip.org/content/aip/journal/apl/106/10?ver=pdfcov>

Published by the [AIP Publishing](#)

Articles you may be interested in

[Photoluminescence of Nd-doped SnO₂ thin films](#)

Appl. Phys. Lett. **100**, 101908 (2012); 10.1063/1.3692747

[Sputtering formation of p-type SnO thin-film transistors on glass toward oxide complimentary circuits](#)

Appl. Phys. Lett. **97**, 072111 (2010); 10.1063/1.3478213

[Carrier relaxation dynamics in Sn x N y nanowires grown by chemical vapor deposition](#)

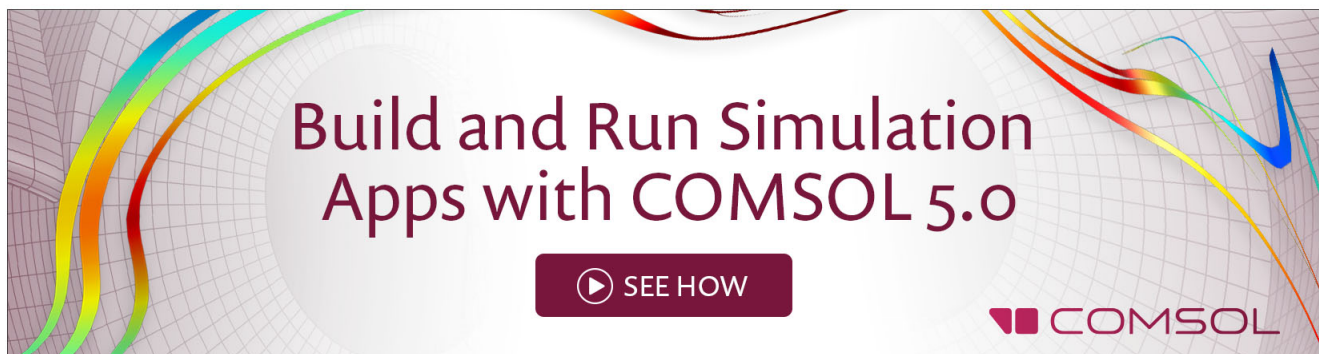
J. Appl. Phys. **106**, 114303 (2009); 10.1063/1.3264721

[Oxygen incorporation in thin films of In₂O₃:Sn prepared by radio frequency sputtering](#)

J. Appl. Phys. **88**, 2437 (2000); 10.1063/1.1287603

[Grain-boundary-limited transport in semiconducting SnO₂ thin films: Model and experiments](#)

J. Appl. Phys. **83**, 888 (1998); 10.1063/1.366773

A promotional banner for COMSOL 5.0. It features a background of a grid with colorful, flowing lines in shades of blue, green, yellow, and red. The text 'Build and Run Simulation Apps with COMSOL 5.0' is centered in a dark red font. Below the text is a dark red button with a white play icon and the text 'SEE HOW'. The COMSOL logo is in the bottom right corner.

Ultrafast carrier dynamics in SnO_x thin films

Zhong-guo Li,¹ Lingyan Liang,^{2,a)} Hongtao Cao,² Zhengguo Xiao,¹ Xingzhi Wu,¹ Yu Fang,³ Junyi Yang,³ Tai-Huei Wei,¹ and Ying-lin Song^{1,3,a)}

¹Department of Physics, Harbin Institute of Technology, Harbin 150001, China

²Division of Functional Materials and Nano Devices, Ningbo Institute of Material Technology and Engineering, Chinese Academy of Sciences, Ningbo 315201, China

³College of Physics, Optoelectronics and Energy, Soochow University, Suzhou 215006, China

(Received 3 February 2015; accepted 2 March 2015; published online 10 March 2015)

We studied the carrier dynamics in a series of SnO_x thin films using femtosecond transient absorption (TA) spectroscopy. The observed carrier relaxation was found to be strongly dependent on thin film stoichiometry. The TA spectra corresponding to free carriers, trapped carriers, and state filling were observed in the picosecond time region for SnO₂, SnO_x, and SnO film, respectively. The TA decay kinetics of all films were best fit with a tri-exponential decay model with fast (1 ps), medium (~10 ps), and slow (ns) components. Our results revealed the carrier relaxation and recombination processes in SnO_x thin films, identifying the critical role of stoichiometry in photo-induced phenomena. © 2015 AIP Publishing LLC.

[<http://dx.doi.org/10.1063/1.4914546>]

Oxide semiconductor materials have garnered tremendous attention in the last decade owing to their diverse applications in transparent electronics, sustainable energy, etc.^{1–3} Among the variety of oxide semiconductors, tin oxide is of special interest because of its excellent stoichiometry flexibility, remarkable microstructure tunability, and wide optical band gap.^{4,5} While the n-type tin dioxide (SnO₂) has been widely explored in various applications, such as solar cells and gas sensors, the p-type tin monoxide (SnO) has received ever-increasing research interest in recent years due to its moderate carrier mobility and unique ambipolar conductivity.^{6–17} A fundamental understanding of the carrier dynamics in photo-excited semiconductor materials is of great importance for improving the efficiency of many optoelectronic and photocatalytic devices.^{18–21} The ultrafast optical spectroscopy (UOS) has been proved to be a very promising tool for studying the thermalization, trapping, and recombination of photo-excited carriers in various oxide semiconductors.^{22–27} Pervious experimental studies revealed that defect states in SnO₂ play a critical role in the carrier decay kinetics, resulting in a sub-nanosecond decay process.^{28,29} However, despite extensive studies of ultrafast carrier recombination in n-type SnO₂ nanostructures,^{30–33} the knowledge of free-carrier dynamics in p-type SnO remains hitherto unclear. Therefore, it is essential to study the ultrafast carrier dynamics in stoichiometric modified SnO_x materials for deeper understanding the fascinating photo-physical properties of tin oxide.

In this letter, the ultrafast carrier dynamics in SnO_x thin films were investigated as a function of compositional variation using femtosecond transient absorption (TA) spectroscopy. The TA spectra of pristine SnO film showed a dominant bleaching peak at ~500 nm, which is attributed to state-filling of optical transition near the band edge. On the contrary, photo-induced absorption by free carrier absorption

and defect-related absorption were observed in the stoichiometric SnO₂ and oxygen deficient SnO_x films. In all films, the photo-excited carriers relaxed over three different time scales and the free carriers showed long lifetimes up to a few nanoseconds. Our results revealed a quantitative picture of carrier relaxation and recombination processes in tin oxide semiconductors, which could be useful for the potential utilization of tin oxide in future device applications.

The SnO_x films used in this study were prepared on quartz glasses using reactive rf magnetron sputtering under various oxygen partial pressure (P_O), with a thickness of ~200 nm. Details about the film fabrication and various property characterizations can be found elsewhere.³⁴ The femtosecond TA spectroscopy was performed using a standard white-light pump-probe measurements. The excitation pulse at 355 nm (3.49 eV) emitted from an optical parametric amplifier pumped by a Yb:KGW femtosecond laser (1.20 eV, 190 fs, and 6 kHz) was chopped with a frequency of 137 Hz and focused loosely on the sample films. The typical pump fluence was <100 μJ/cm². The white-light probe pulse was generated by focusing a 1.2 eV laser pulse onto a sapphire plate. The transmitted probe pulse after the sample films was detected by a Si photodetector after a monochromator. The differential transmittance signals, ΔOD, were obtained by comparing the transmittance of probe pulses with and without the pump pulses using lock-in detection. The temporal resolution of the measurement system was ~280 fs. All measurements were performed at room temperature. Further details can be found in Ref. 35.

Figure 1(a) shows the XRD patterns of the SnO_x films at various P_O . At low P_O , clear XRD peaks were observed, which can be unambiguously assigned to those of the α-SnO crystal structure (P4/nmm, JCPDS card No. 06-0395). Further increasing the P_O above 10.7%, the XRD patterns became broad and featureless, indicating the amorphous nature of the films. This result is consistent with the previous report.^{34,36} The crystallinity of the films were elucidated based on the XRD data to be nanocrystalline, amorphous,

^{a)}Authors to whom correspondence should be addressed. Electronic addresses: ylsong@hit.edu.cn and lly@nimte.ac.cn.

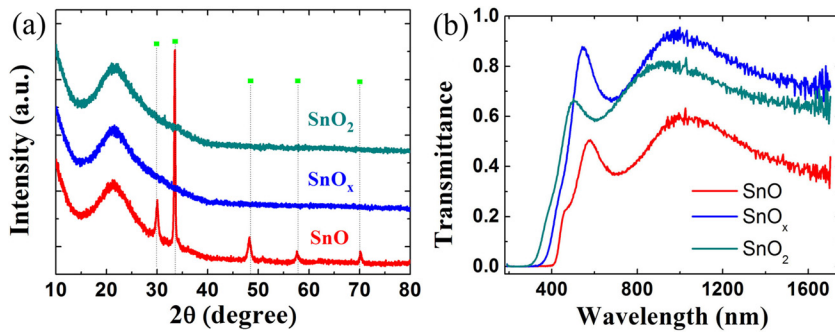


FIG. 1. (a) XRD patterns of the SnO_2 , SnO_x , and SnO films deposited with different oxygen pressure (P_{O}). The dotted lines indicate the α - SnO phase (space group: $P4/nmm$). (b) The transmittance spectra of the SnO_x films.

and polycrystalline for SnO_2 , SnO_x , and SnO , respectively. Figure 1(b) presents the linear transmittance spectra of the SnO_x films. As the P_{O} increased, the optical bandgap of the SnO_x films increases continuously from ~ 2.86 eV to 3.7 eV, which is in a good agreement with the previous report.^{15,34,37} Furthermore, the optical transmittance spectra clearly demonstrate that there is absorption below the band edge, which is related to the shallow defect state within the band gap.

Figure 2 illustrates the typical TA spectra of SnO_2 , SnO_x , and SnO films at various time delays under 355 nm pulses excitation, respectively. The pump photon energy (3.49 eV) was utilized to near resonance with or higher than the band gap energy of the tin oxide films. To eliminate the possible effect of excitation photon energy on carrier dynamics, femtosecond pump-probe measurements were carried out with 2.41 eV (515 nm) photons corresponding to two-photon absorption well above the band edge. The results appear to be identical with the data under 3.49 eV excitation. In order to avoid second-order charge recombination, all the measurements were performed by keeping the laser fluence less than $30 \mu\text{J}/\text{cm}^2$. In the SnO_2 film, we observed a Drude-like free carrier response and a broad absorption peak centered at 530 nm (2.34 eV) almost immediately after excitation. This absorption band is consistent with the previous photoluminescence (PL) experiment, which is ascribed to defect state in the bandgap of SnO_2 .³⁸ It is worth noticing that the observed spectral change is analogous to that of the benchmark oxide semiconductors TiO_2 , indicating carrier relaxation in the nanocrystalline SnO_2 film is similar to the nanocrystalline TiO_2 .^{22–24} As the delay time increases, the

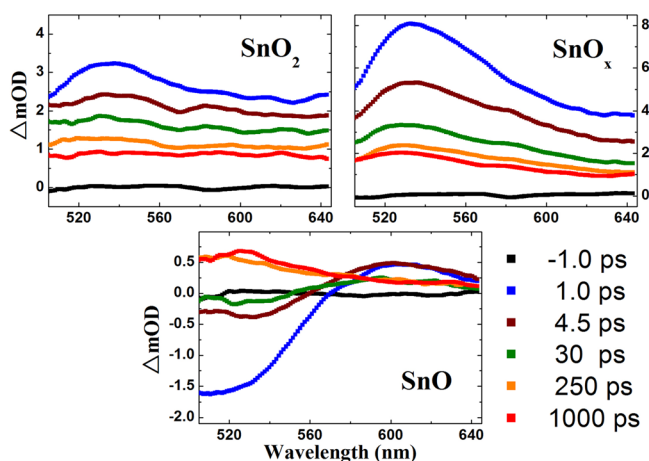


FIG. 2. Transient absorption spectra of the SnO_2 , SnO_x , and SnO films excited with 355 nm (3.49 eV) laser pulses at fluence of $14 \mu\text{J}/\text{cm}^2$.

2.34 eV absorption band rapidly broadens and vanishes after tens of picoseconds, leaving a broad and featureless TA spectrum persists up to a few nanoseconds. In the oxygen deficient SnO_x film, the strong absorption band at 530 nm can be clearly identified at very early time delays. This result indicates that a large number of defect states form in the amorphous SnO_x film, which effectively trap the photo-excited carriers. With an increase in the delay time, the 530 nm absorption band shows a small blueshift, which could be attributed to the crossover between shallow defect state near the band edge to deep defect state located in the forbidden gap.²⁶ Contrary to the SnO_2 film, the relaxation of the 530 nm absorption band proceeds much slowly in the SnO_x film. After 30 ps, a distinct TA signal is still observable over the whole spectrum. Then, the spectrum gradually loses its structure in about hundreds of picoseconds. Finally, only a large and featureless continuum and a faint absorption band signal are detectable for time delays up to nanosecond regime. This result indicates that the carrier lifetime is rather long in the SnO_x film. In polycrystalline SnO film, however, laser excitation leads to an instantaneous buildup of bleaching feature with maximum at ~ 500 nm (2.49 eV), while a positive absorption signal in the 570–640 nm region is evident which is attributed to free carrier absorption. The observed bleaching of interband transition is smaller than the optical band gap determined by linear transmittance measurement, which indicates the defect-related bleaching is dominant in the visible regime. The amplitude of TA signal indicates that the concentration of defect states in the polycrystalline SnO film is smaller than the amorphous SnO_2 or SnO_x films, which is consistent with the previous PL measurements.^{10,38} Following the intense bleaching, the TA spectrum decays within tens of picoseconds, resulting in a nearly featureless and positive continuum which extends over the entire investigated spectral range after 250 ps time delay. The quartz substrate was also measured under the same experimental conditions and found to have negligible response. We confirmed that no photo-induced damage of the sample was observed during our experiments, and the TA signal is repeatable at different spot of the SnO_x films.

The normalized TA decay dynamics of SnO_2 , SnO_x , and SnO films are shown in Figs. 3(a)–3(c) for a probe photon energy of 2.33 eV, respectively. For all of the samples studied, no excitation-intensity-dependent decay process was observed until the pump fluence was larger than $46 \mu\text{J}/\text{cm}^2$. Othonos *et al.* reported the intensity threshold for high order effects such as Auger recombination take place at $50 \mu\text{J}/\text{cm}^2$ for SnO_2 nanowires.²⁸ Therefore, our measurements were

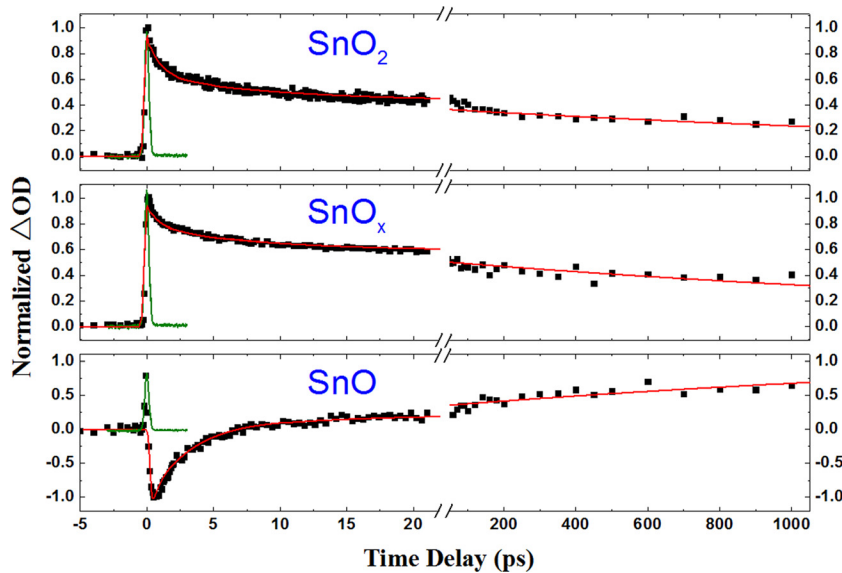


FIG. 3. Normalized transient absorption decay dynamics extracted at 2.33 eV (532 nm) for (a) SnO₂, (b) SnO_x, and (c) SnO films under weak excitation conditions, respectively. The red lines are theoretical fitting results. The green curves represent the instrument response function.

conducted in the low perturbation regime. The decay curves show a pulse-width-limited instantaneous rise, followed by a multi-exponential recovery. This characteristic behavior is observed for all probing wavelengths. The first 20 ps decay dynamics of all three films are composed of a fast and a slow decay component with time constants τ_1 of 1 ps and τ_2 of tens of picoseconds, respectively. And the carrier decay in long time scale was rather slow with lifetime τ_3 of up to a few nanoseconds. The experimental data can be fitted by a convolution between the instrument response function and a tri-exponential decay model

$$\Delta T(t) = R_{IRF} \otimes \left[\sum_{i=1,3} A_i \exp\left(-\frac{t}{\tau_i}\right) \right], \quad (1)$$

where $\Delta T(t)$ is the normalized transmittance change, R_{IRF} is the instrument response function, τ_i and A_i are the time constants and amplitudes, respectively. The fitting parameters obtained for the three films are summarized in Table I. The relative uncertainty for both decay times and amplitudes is $\sim 15\%$. It can be found that the model fits the experimental data very well.

Here, we consider the origin of the observed carrier recombination dynamics in tin oxide films. It is known that photo-generated carriers can follow different decay pathways, which depends on crystallinity and stoichiometry of the semiconductor materials. In amorphous SnO₂ and SnO_x films, the TA signal due to free carrier absorption and defect-related absorption appears immediately after pump excitation, indicating that the thermalization of hot photo-excited carriers via carrier-carrier scattering and defect trapping is accomplished on the order of hundreds of

femtoseconds. Similar ultrafast carrier relaxation was also reported for other oxides.^{22,24} The fast decay component (~ 1 ps) was observed for both films and found to be power-independent under our experimental conditions. This result indicates that the high order carrier-carrier interaction processes such as Auger recombination are not important. Therefore, we attribute the fast decay to the redistribution of photo-generated carriers among the shallow defect states below the band edge. The relatively slow decay component could be assigned to the nonradiative relaxation of carriers toward deeper trap states in the band gap. Finally, the long decay component is related to the carrier recombination from this deep trap state to the valence band. The timescale we observed is analogous to the carrier relaxation time in SnO₂ nanowires reported by Othonos *et al.*²⁸ And similar carrier decay process has been recently observed in other semiconductor materials.^{39,40} In the polycrystalline SnO film, the negative TA signal peaking at ~ 500 nm emerges at very early time delays, which is attributed to the ultrafast bleaching of the defect state. After photo-excitation, the relaxation of bleaching on a few picoseconds time scale is assigned to the cooling of hot carriers to the band edge or shallow defect state. Similar to the SnO₂ and SnO_x cases, these shallow trapped carriers gradually relax into deep trap states on 10 ps time scale. These trapped carriers have a long lifetime (~ 2 ns), and thermal activation of carriers in the trap states induces absorption signal up to a few nanoseconds. Regardless of the decay mechanisms, we note that at least 24% of photo-excited carriers in all three films remain for time delay longer than 1 ns. The observed long lifetime of carriers is extremely useful for photocatalytic and transparent electronics applications. Therefore, our results demonstrate that the sputtered SnO_x thin films are promising candidate materials for applications in solar cells, thin film transistors, sensor, etc.

In summary, we studied the ultrafast carrier dynamics of SnO₂, SnO_x, and SnO thin films prepared by magnetron sputtering using femtosecond transient absorption measurements. The thin film stoichiometry was found to play a critical role in determining the optical properties and dynamics of photo-

TABLE I. Summary of fitting parameters for transient absorption dynamics of tin oxide films.

	A_1	τ_1 (ps)	A_2	τ_2 (ps)	A_3	τ_3 (ns)
SnO ₂	0.59	1.0	0.16	9.5	0.22	2.2
SnO _x	0.48	1.2	0.18	12.0	0.29	1.8
SnO	0.51	1.3	0.23	10.5	0.22	1.9

generated carriers. The transient absorption signals corresponding to the free carrier absorption, defect-related absorption, and photo-bleaching were observed in SnO₂, SnO_x, and SnO films, respectively. Kinetics of these transients was fitted well with a multi-exponential decay model with fast (~1 ps), medium (~10 ps), and long (ns) time constants under weak excitation fluence conditions. Our results elucidate the carrier relaxation mechanism of tin oxide materials, which is necessary for further optimizing the operation of SnO-based devices.

The authors acknowledge the support of the Chinese National Program on Key Basic Research Project (2012CB933003), and the National Natural Science Foundation of China (Grant No. 11104289 and 61274095).

- ¹K. Nomura, H. Ohta, A. Takagi, T. Kamiya, M. Hirano, and H. Hosono, *Nature* **432**, 488 (2004).
- ²E. Fortunato, P. Barquinha, and R. Martins, *Adv. Mater.* **24**, 2945 (2012).
- ³L. Sang, Y. Zhao, and C. Burda, *Chem. Rev.* **114**, 9283 (2014).
- ⁴D. S. Ginley, H. Hosono, and D. C. Paine, *Handbook of Transparent Conductors* (Springer, Berlin, 2010), Chap. 6.
- ⁵M. Batzill and U. Diebold, *Prog. Surf. Sci.* **79**, 47 (2005).
- ⁶Y. Ogo, H. Hiramatsu, K. Nomura, H. Yanagi, T. Kamiya, M. Hirano, and H. Hosono, *Appl. Phys. Lett.* **93**, 032113 (2008).
- ⁷K. Nomura, T. Kamiya, and H. Hosono, *Adv. Mater.* **23**, 3431 (2011).
- ⁸E. Fortunato, R. Barros, P. Barquinha, V. Figueiredo, S. K. Park, C. S. Hwang, and R. Martins, *Appl. Phys. Lett.* **97**, 052105 (2010).
- ⁹L. Y. Liang, Z. M. Liu, H. T. Cao, and X. Q. Pan, *ACS Appl. Mater. Interfaces* **2**, 1060 (2010).
- ¹⁰W. Guo, L. Fu, Y. Zhang, K. Zhang, L. Y. Liang, Z. M. Liu, H. T. Cao, and X. Q. Pan, *Appl. Phys. Lett.* **96**, 042113 (2010).
- ¹¹L. Y. Liang, H. T. Cao, X. B. Chen, Z. M. Liu, F. Zhuge, H. Luo, J. Li, Y. C. Lu, and W. Lu, *Appl. Phys. Lett.* **100**, 263502 (2012).
- ¹²J. A. Caraveo-Frescas, P. K. Nayak, H. A. Al-Jawhari, D. B. Granato, U. Schwingenschlogl, and H. N. Alshareef, *ACS Nano* **7**, 5160 (2013).
- ¹³J. A. Caraveo-Frescas, M. A. Khan, and H. N. Alshareef, *Sci. Rep.* **4**, 5243 (2014).
- ¹⁴M. K. Hota, J. A. Caraveo-Frescas, M. A. McLachlan, and H. N. Alshareef, *Appl. Phys. Lett.* **104**, 152104 (2014).
- ¹⁵N. F. Quackenbush, J. P. Allen, D. O. Scanlon, S. Sallis, J. A. Hewlett, A. S. Nandur, B. Chen, K. E. Smith, C. Weiland, D. A. Fischer, J. C. Woicik, B. E. White, G. W. Watson, and L. F. J. Piper, *Chem. Mater.* **25**, 3114 (2013).
- ¹⁶H. N. Lee, H. J. Kim, and C. K. Kim, *Jpn. J. Appl. Phys., Part 1* **49**, 020202 (2010).
- ¹⁷J. H. Han, Y. J. Chung, B. K. Park, S. K. Kim, H. S. Kim, C. G. Kim, and T. M. Chung, *Chem. Mater.* **26**, 6088 (2014).
- ¹⁸A. Othonos, *J. Appl. Phys.* **83**, 1789 (1998).
- ¹⁹V. I. Klimov, *J. Phys. Chem. B* **104**, 6112 (2000).
- ²⁰D. A. Wheeler and J. Z. Zhang, *Adv. Mater.* **25**, 2878 (2013).
- ²¹J. B. Baxter, C. Richter, and C. A. Schmuttenmaer, *Annu. Rev. Phys. Chem.* **65**, 423 (2014).
- ²²Y. Tamaki, A. Furube, M. Murai, K. Hara, R. Katoh, and M. Tachiya, *Phys. Chem. Chem. Phys.* **9**, 1453 (2007).
- ²³D. A. Wheeler, Y. Ling, R. J. Dillon, R. C. Fitzmorris, C. G. Dudzik, L. Zavodivker, T. Rajh, N. M. Dimitrijevic, G. Millhauser, C. Bardeen, Y. Li, and J. Z. Zhang, *J. Phys. Chem. C* **117**, 26821 (2013).
- ²⁴L. Triggiani, A. Brunetti, A. Aloï, R. Comparelli, M. L. Curri, A. Agostiano, M. Striccoli, and R. Tommasi, *J. Phys. Chem. C* **118**, 25215 (2014).
- ²⁵T. Shin, E. Lee, S. Sul, H. Lee, D. S. Ko, A. Benayad, H. S. Kim, and G. S. Park, *Opt. Lett.* **39**, 5062 (2014).
- ²⁶Y. Yamada, T. Nakamura, S. Yasui, H. Funakubo, and Y. Kanemitsu, *Phys. Rev. B* **89**, 035133 (2014).
- ²⁷S. Y. Smolin, M. D. Scafetta, G. W. Guglietta, J. B. Baxter, and S. J. May, *Appl. Phys. Lett.* **105**, 022103 (2014).
- ²⁸A. Othonos, M. Zervos, and D. Tsokkou, *Nanoscale Res. Lett.* **4**, 828 (2009).
- ²⁹A. Kar, M. A. Stroschio, M. Meyyappan, D. J. Gosztola, G. P. Wiederrecht, and M. Dutta, *Nanotechnology* **22**, 285709 (2011).
- ³⁰J. J. Cavaleri, D. P. Colombo, Jr., and R. M. Bowman, *J. Phys. Chem. B* **102**, 1341 (1998).
- ³¹K. Tvrđy, P. A. Frantsuzov, and P. V. Kamat, *Proc. Natl. Acad. Sci. U.S.A.* **108**, 29 (2011).
- ³²P. Tiwana, P. Docampo, M. B. Johnston, H. J. Snaith, and L. M. Herz, *ACS Nano* **5**, 5158 (2011).
- ³³D. Tsokkou, A. Othonos, and M. Zervos, *Appl. Phys. Lett.* **100**, 133101 (2012).
- ³⁴H. Luo, L. Y. Liang, H. T. Cao, Z. M. Liu, and F. Zhuge, *ACS Appl. Mater. Interfaces* **4**, 5673 (2012).
- ³⁵Z. G. Li, R. Zhao, W. W. Li, H. Y. Wang, H. Yang, and Y. L. Song, *Appl. Phys. Lett.* **105**, 162904 (2014).
- ³⁶P. C. Hsu, C. J. Hsu, C. H. Chang, S. P. Tsai, W. C. Chen, H. H. Hsieh, and C. C. Wu, *ACS Appl. Mater. Interfaces* **6**, 13724 (2014).
- ³⁷T. Toyama, Y. Seo, T. Konishi, H. Okamoto, R. Morimoto, Y. Nishikawa, and Y. Tsutsumi, *Thin Solid Films* **555**, 148 (2014).
- ³⁸A. Kar, M. A. Stroschio, M. Dutta, J. Kumari, and M. Meyyappan, *Appl. Phys. Lett.* **94**, 101905 (2009).
- ³⁹L. Q. Phuong, M. Okano, Y. Yamada, G. Yamashita, T. Morimoto, M. Nagai, M. Ashida, A. Nagaoka, K. Yoshino, and Y. Kanemitsu, *Appl. Phys. Lett.* **105**, 231902 (2014).
- ⁴⁰C. Y. Yang, C. T. Chia, H. Y. Chen, S. Gwo, and K. H. Lin, *Appl. Phys. Lett.* **105**, 212105 (2014).